agronomy

MDPI

Article

A Novel Pesticide Vectorization Strategy: Development of Phloem-Mobile PCA Amide Derivatives for Enhanced Crop Disease Control

Li Li [1], Yao Tian [1], Guoqing Mao [1], Tingyu Yu [1], Qian Huang [1,2], Linhua Yu [1], Xiang Zhu [1,3,*] and Junkai Li [1,*]

[1] MARA Key Laboratory of Sustainable Crop Production in the Middle Reaches of the Yangtze River (Co-Construction by Ministry and Province), Hubei Key Laboratory of Waterlogging Disaster and Agricultural Use of Wetland, College of Agriculture, Yangtze University, Jingmi Road 88, Jingzhou 434025, China; bohecha901@sina.com (L.L.); yaotien@163.com (Y.T.); maoguoqing1688@163.com (G.M.); y18672395703@163.com (T.Y.); huangqian2025@foxmail.com (Q.H.); linhuayu531@sina.com (L.Y.)
[2] Plant Protection Research Institute, Guangxi Academy of Agricultural Sciences, Nanning 530007, China
[3] National Key Laboratory of Green Pesticide, Ministry of Education, Guizhou University, Guiyang 550025, China
* Correspondence: xiangzhu1992@yangtzeu.edu.cn (X.Z.); junkaili@sina.com (J.L.); Tel./Fax: +86-716-8066314 (X.Z.); +86-716-8066767 (J.L.)

Abstract

The phloem mobility of fungicides is a highly advantageous property for controlling plant root and vascular diseases. In order to develop phloem-mobile fungicides with enhanced antifungal activity, a new pesticide vectorization strategy was proposed for using exogenous compounds as vector groups in this study. Nine novel PCA amide derivatives containing heterocyclic carboxylic acids were designed and synthesized by coupling PCA with a heterocyclic carboxylic acid via an amide linkage. In vitro bioassays revealed that nine target compounds exhibited moderate to strong antifungal activity against the tested fungal pathogens. Notably, compound **D4** demonstrated superior inhibitory effects against multiple pathogenic fungi. The results of phloem mobility tests demonstrated that five target compounds, **D1**, **D2**, **D4**, **D7**, and **D9**, exhibited phloem mobility, which is consistent with possible carrier-mediated transport. In pot experiments, compound **D4** exhibited significantly better protective and curative efficacy against rice sheath blight than PCA, a benefit that may stem from its phloem mobility. Further systemic translocation studies in tobacco (*Nicotiana tabacum* L.) confirmed that compound **D4** is readily absorbed by leaves and efficiently distributed throughout the plant, with pronounced accumulation in roots and stems. This translocation pattern may play a significant role in improving the effectiveness of compound **D4** in controlling root and vascular diseases.

Keywords: synthesis; phloem mobility; heterocyclic carboxylic acid; carrier-mediated transport; antifungal activities; phenazine-1-carboxylic acid (PCA); systemic fungicide; vectorization strategy

Academic Editors: Rosa M. Varela, Jesús G. Zorrilla and Francisco J.R. Mejías

Received: 21 August 2026
Revised: 8 September 2026
Accepted: 8 September 2026
Published: 9 September 2026

1. Introduction

Plant pests and diseases cause a significant reduction in crop yields and a deterioration in food quality, thereby posing a major threat to agricultural production globally [1,2]. Chemical pesticides, known for their rapidity, high efficiency, and cost-effectiveness, have become the primary method for controlling crop pests and diseases in modern agriculture [3,4]. In recent years, as intensive and large-scale agricultural practices have

expanded in China, the application of drones for precise pesticide spraying to control pests and diseases has progressively emerged as a standard practice and a critical trend for the future agriculture [5–7]. Although this method has markedly enhanced production efficiency, limitations such as crop density, canopy structure, and environmental factors often prevent pesticides from directly reaching the parts of plants damaged by pests or diseases, thus decreasing control efficacy [8–10]. Phloem systemic pesticides possess the advantageous property of being absorbed via foliar application and translocated throughout the entire plant, achieving overall protection for crops [11,12]. However, the varieties of this type of pesticides are still very limited, such as oxathiapiprolin [13], metalaxyl [14], and spirotetramat [15]. Therefore, it is extremely urgent to strengthen the theoretical and developmental research of phloem systemic pesticides.

The plant cuticle constitutes the first barrier encountered by pesticides before their absorption into crop leaves [16–18]. Facilitated by adjuvants, however, most pesticides can diffuse through this layer to varying degrees. Subsequently, the plasma membrane forms the second physical barrier that pesticides must overcome to enter the sap flow and undergo phloem movement within the plant [19–21]. Early research indicates that exogenous compounds with appropriate physicochemical properties, such as the octanol–water partition coefficient (Log*K*ow) and acid dissociation constant (p*K*a), can cross biological membranes via passive diffusion or ion-trapping mechanisms [22–24]. Advances in modern molecular biology have revealed that some other pesticides can utilize specific transport proteins on the plasma membrane for crossing via active transport [25,26]. This way enables their long-distance movement. For example, glyphosate utilizes the phosphate transport protein, while paraquat utilizes the polyamine transport protein [27,28].

In recent years, a pesticide vectorization strategy has been proposed to develop phloem systemic pesticides, based on understanding exogenous substance transmembrane transport mechanisms [29]. This strategy involves conjugating a non-systemic pesticide with a nutrient (α-amino acids or sugars); the resulting conjugate may then be actively transported across the plasma membrane via nutrient-specific transporters [30,31]. For example, Xu-Hanhong's group conjugated glucose to the insecticide fipronil, yielding GTF (Figure 1), which showed excellent phloem mobility in castor bean seedlings via a sugar transporter system. However, the insecticidal activity of GTF against third-instar larvae of *Plutella xylostella* within 24 h was reduced by 7–8-fold [32,33]. Similar results occur with other pesticide–nutrient conjugates. Yu et al. coupled L-amino acids with a non-systemic biofungicide shenqinmycin (chemical name: phenazine-1-carboxylic acid, PCA; Figure 1), obtaining a series of PCA–amino acid conjugates, and most of the conjugates displayed excellent phloem mobility [34,35]. PCA-L-Val (Figure 1) was absorbed by tobacco leaves, transported basipetally to roots for accumulation, and partially reconverted to PCA [19]. Its uptake and transport in castor plants involves active transport by multiple amino acid transporters [36]. Yang et al. conjugated carbendazim with auxin indoleacetic acid (IAA) to form IAAC (Figure 1). IAAC achieved phloem mobility in soybean seedlings while retaining IAA's plant-growth-stimulating properties [37].

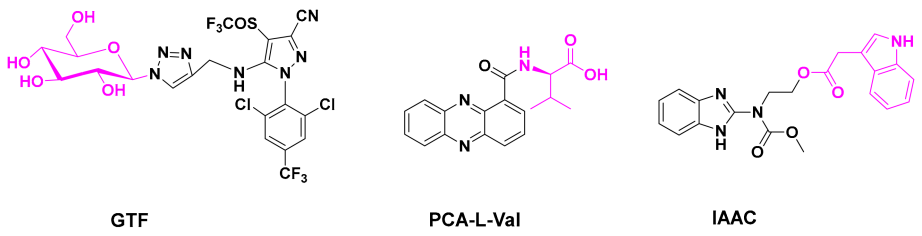

Figure 1. Structures of pesticide–nutrient conjugates.

The aforementioned results have confirmed the feasibility of the vectorization strategy in enhancing the phloem systemicity of pesticides. However, since nutrients are derived from plant tissues and typically possess specific physiological and biochemical functions, this often compromises both the chemical stability and pesticidal activity of pesticide–nutrient conjugates [32–34]. Therefore, how to achieve phloem mobility while enhancing its pesticidal activity constitutes a key challenge that needs to be addressed. Therefore, we hypothesize that if endogenous nutrients can serve as vector groups, then some exogenous phloem-mobile chemical structures may also serve as vector groups to achieve this goal. A number of synthetic herbicides with excellent phloem systemic mobility—such as benzoic acids, imidazolinones, quinoline carboxylic acids, pyridinecarboxylic acids, and sulfonylureas—have attracted our attention [38–40]. Some representative compounds are listed in Figure 2. It is noteworthy that although these herbicides vary in their target sites, they exhibit considerable structural similarity by typically containing characteristic aromatic (or heterocyclic) carboxylic acid motifs, which may constitute the key structural basis for their phloem mobility.

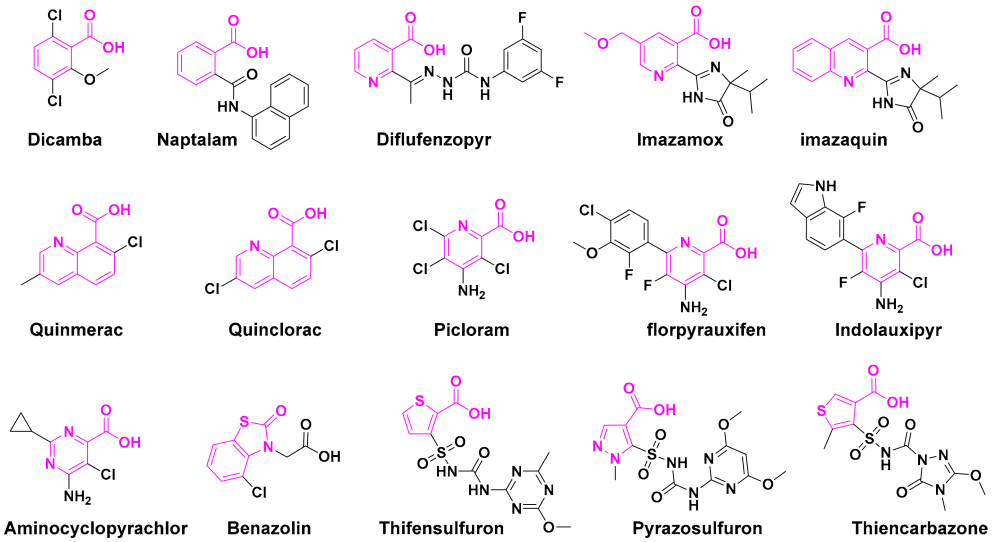

Figure 2. Chemical structures of some representative systemic herbicides.

To verify our hypothesis that exogenous chemical structures can serve as vector groups in pesticide vectorization strategy, the following studies were conducted in this work. We first assessed the phloem mobility of nine commercially available heterocyclic carboxylic acid compounds using the *Ricinus communis* system. Using these small molecules as vector groups, we conjugated each of them with the non-systemic biofungicide PCA via an amide bond, obtaining nine corresponding conjugates. The phloem mobility and antifungal activity of these conjugates were systematically evaluated. These findings will contribute to a deeper understanding and advancement of theoretical research on pesticide vectorization, while also providing data support for the development of phloem-mobile pesticides with enhanced bioactivity.

2. Materials and Methods

2.1. Chemicals and Instruments

Phenazine-1-carboxylic acid (PCA) was provided by the College of Agriculture, Yangtze University. All chemicals and solvents were commercially available and used without further purification. Reaction progress was monitored by thin-layer chromatography (TLC) using silica gel GF254 (Qingdao Ocean Chemical Co., Ltd., Qingdao, China). Target compounds were purified by silica gel column chromatography (200–300 mesh,

Qingdao Ocean Chemical Co., Ltd., Qingdao, China). ^{1}H NMR and ^{13}C NMR spectra were recorded on an AVANCE DPX400 spectrometer (Bruker Spectrospin, Ettlingen, Germany) using deuterated dimethyl sulfoxide (DMSO-d_6), deuterated chloroform ($CDCl_3$), or deuterated trifluoroacetic acid (TFA-*d*) as solvents, with tetramethylsilane (TMS) as the internal standard. High-resolution mass spectrometry (HRMS) data were acquired on a Thermo Scientific Q Exactive mass spectrometer (Thermo Fisher Scientific, Waltham, MA, USA). The melting points of all target compounds were determined using a WRR melting point apparatus (Shanghai Jingke Industrial Co., Ltd., Shanghai, China) without correction.

2.2. Plant Materials and Pathogens

Castor seedlings. Mature castor (*Ricinus communis* L.) seeds (provided by the Zibo Academy of Agricultural Sciences, Zibo, China) were soaked for 48 h until germination initiated. After radicle emergence, the seeds were germinated at 28 °C for 48 h. Germinated seeds were selected and sown in a nursery substrate with sufficient moisture. The growth conditions were maintained at 80% relative humidity, 28 °C, and a 14 h/10 h light/dark cycle in an artificial climate chamber. Seedlings were harvested 6 days after sowing, prior to cotyledon emergence from the endosperm.

Tobacco seedlings. Tobacco (*Nicotiana tabacum* L.) seeds (cultivar Yunyan 87, provided by the Guizhou Academy of Tobacco Science, Guizhou, China) were sown in nutrient pots filled with nutrient-rich, easily wettable growth substrate, (3–4 seeds per pot, sown per pot at a depth of approximately 0.5 cm). After approximately one month of growth at room temperature, healthy and uniformly developed seedlings were selected and transplanted to experimental plots. The plants were further cultivated until reaching the 8–10 leaf stage for use in experiment.

Rice (*Oryza sativa* L.) seedlings. Rice seeds (cultivar 'Yangshanyou 48' provided by the Agricultural Laboratory of Yangtze University, Jingzhou, China) were first immersed in 40 °C warm water for 10 min, then drained and soaked in water at room temperature for 24 h until germination initiated. The pre-germinated seeds were incubated at 28 °C in the dark to promote sprouting. Well-sprouted seeds (with both radicle and coleoptile developed) were selected and sown in pots (20 seeds per pot) covered with a thin layer of soil, and kept moist. When the seedlings reached the two-leaf-one-heart stage, they were thinned to 12 plants per pot and transferred to a greenhouse for further growth. The plants were cultivated until the early tillering stage before being labeled for experimentation.

Pathogenic fungi. Eight phytopathogenic fungi species, *Rhizoctonia solani* (YZUP22101), *Fusarium moniliforme* (YZUP23005), *Pythium debaryanum* (YZUP23028), *Botrytis cinerea* (YZUP22501), *Phytophthora infestans* (YZUP24098), *Bipolaris maydis* (YZUP24082), *Colletotrichum camelliae* (YZUP23035), and *Myricularia oryzae* (YZUP23103), were provided by Plant Pathology Laboratory, College of Agriculture, Yangtze University. These fungi were maintained on potato dextrose agar (PDA) medium at 4 °C.

2.3. Collection and Analysis of Phloem Sap

Phloem Sap Collection. The phloem mobility of the compounds was evaluated using a castor seedling system, following a previously described method [33,34]. The endosperm was carefully removed from the seedlings without damaging the cotyledons, and the roots were thoroughly rinsed. The cotyledons were then immersed in a buffer solution (pH 5.5) containing 0.1% Tween 80, 2 mL *N*, *N*-dimethylformamide (DMF), 5 mL of 200 mmol/L Na_2HPO_4, 92 mL of 500 mmol/L NaH_2PO_4, and 200 μmol/L of each test compound. The roots were immersed in distilled water containing 0.5 mmol/L $CaCl_2$. Deionized water was used as the control. The test concentration of 200 μmol/L and the pH 5.5 phosphate buffer system were selected according to previously reported *R. communis* phloem mobility

assays to ensure sufficient analytical sensitivity and maintain comparable experimental conditions. Tween 80 and a small amount of DMF were used to improve wetting and solubilization of the tested compounds. After 2 h of incubation in the treatment buffer, the seedlings were excised 1 cm below the cotyledonary node, and the roots were discarded. Phloem sap exuding from the cut surface was collected at 1 h, 2 h, 3 h, 4 h, and 5 h intervals. The collected sap was diluted threefold with deionized water, filtered through a 0.22 μm aqueous-phase microporous membrane, and stored for subsequent analysis. The collected sap was diluted threefold with deionized water and filtered through a 0.22 μm hydrophilic nylon syringe filter before analysis.

Analytical method. The processed phloem sap samples were analyzed using a Thermo UltiMate 3000 TSQ-Quantis HPLC-MS system (Waltham, MA, USA). Separation was performed on an Agilent C18 reversed-phase column (5 μm, 150 × 4.6 mm i.d.) maintained at 40 °C. The mobile phase consisted of methanol and 0.1% aqueous formic acid (80:20, v/v) delivered at a flow rate of 0.3 mL/min. The injection volume was 2 μL. Quantification was carried out using an external standard method. A series of standard solutions with gradient concentrations (e.g., 50.00, 25.00, 12.50, 6.25, 3.13, 1.56, 0.78 μmol/L) were prepared by dissolving the target compounds in methanol. The peak areas of the standard solutions and samples were measured under the same chromatographic conditions. A calibration curve was constructed by plotting the peak area against the concentration of the standard solutions, and the content of each compound in the samples was calculated based on the regression equation.

2.4. Synthesis

The synthetic route of the target compounds **D1**–**D9** are outlined in Figure 3.

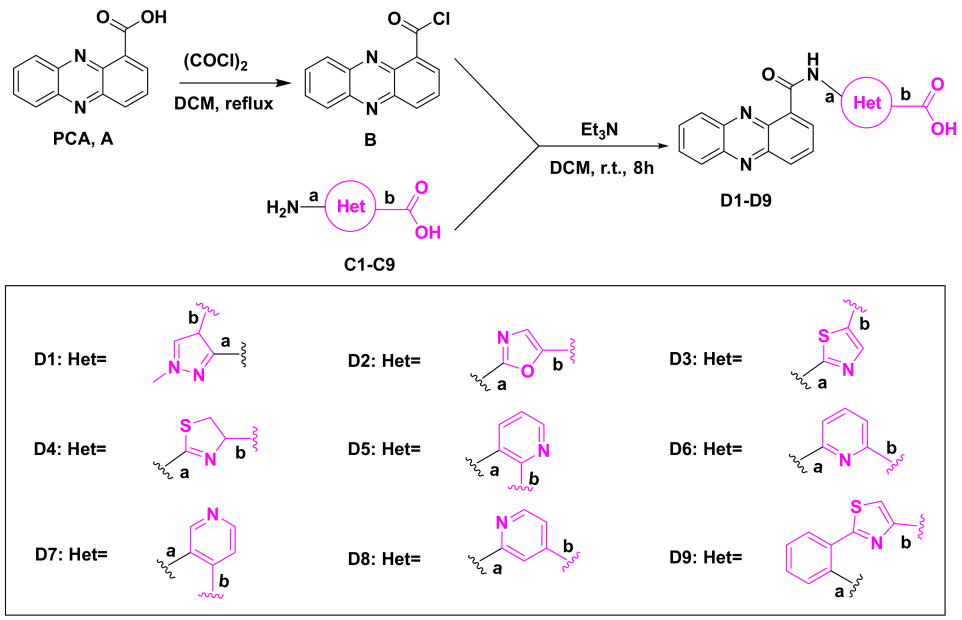

Figure 3. The synthetic route to the target PCA amide derivatives **D1**–**D9**.

General Procedure for Synthesis of Intermediate B. Intermediate **B** was synthesized as previously described [33]. PCA (0.9 g, 8 mmol) was added to a flask containing 30 mL of anhydrous dichloromethane (CH_2Cl_2). Oxalyl chloride (4 mL) and DMF (2–3 drops) were then added dropwise sequentially to the reaction mixture at room temperature. After stabilization, the mixture was refluxed for 2–3 h while monitoring the reaction progress by thin-layer chromatography (TLC). Upon completion, the solvent was removed under

reduced pressure at 65 °C using a rotary evaporator to afford the crude intermediate **B**, which was used directly in the next step without further purification.

General Procedure for Synthesis of Target Compounds D1–D9. The corresponding heterocyclic acid **C** (10 mmol) was slowly added to a solution of intermediate **B** (8 mmol) in anhydrous CH_2Cl_2 (30 mL) under an inert atmosphere. Triethylamine (30 mmol) was then introduced as an acid scavenger, and the reaction mixture was stirred at room temperature for 8 h. Upon completion (monitored by TLC), the solvent was removed under reduced pressure at 40 °C using a rotary evaporator. The crude residue was treated with dilute hydrochloric acid, and the resulting precipitate was collected by filtration. The crude product was then purified through recrystallization to afford compounds **D1–D9**. The spectral data of representative target compounds **D1** and **D2** are shown below. The characterization data and spectra of compounds **D3–D9** are provided in the corresponding figures in the Supporting Information.

1-Methyl-3-(phenazine-1-carboxamido)-1*H*-pyrazole-4-carboxylic acid (**D1**), yellowish green solid, mp > 200 °C. ^{1}H NMR (400 MHz, DMSO-d_6) δ 13.30 (s, 1H), 8.89 (dd, *J* = 7.2, 1.5 Hz, 1H), 8.82 (dq, *J* = 7.4, 2.9 Hz, 1H), 8.47 (dd, *J* = 8.6, 1.6 Hz, 1H), 8.31–8.26 (m, 1H), 8.24 (s, 1H), 8.12 (dd, *J* = 8.7, 7.2 Hz, 1H), 8.06–7.99 (m, 2H), 3.88 (s, 3H). ^{13}C NMR (101 MHz, TFA-$_1$) δ 164.25, 164.20, 145.72, 144.16, 142.10, 141.72, 140.06, 138.99, 138.08, 136.00, 132.16, 131.39, 130.97, 127.11, 126.59, 120.32, 102.66, 39.20. HRMS (ESI): calcd for $C_{18}H_{13}N_5O_3$ $[M+H]^+$, 348.1091; found, 348.1092.

2-(Phenazine-1-carboxamido)oxazole-5-carboxylic acid (**D2**), brownish yellow solid, mp > 200 °C. ^{1}H NMR (400 MHz, DMSO-d_6) δ 13.45 (s, 1H), 8.62 (d, *J* = 7.0 Hz, 1H), 8.53 (dd, *J* = 8.8, 1.4 Hz, 1H), 8.37–8.33 (m, 1H), 8.32–8.28 (m, 1H), 8.16–8.06 (m, 3H), 7.88 (s, 1H). ^{13}C NMR (101 MHz, TFA-$_1$) δ 162.45, 158.50, 154.40, 144.07, 141.08, 141.02, 140.66, 138.65, 137.32, 136.64, 133.77, 132.79, 129.61, 128.62, 124.82, 124.35, 121.38. HRMS (ESI): calcd for $C_{17}H_{10}N_4O_4$ $[M+H]^+$, 335.0775; found, 335.0778.

2.5. Physicochemical Properties of the Compounds

To investigate the relationship between the physicochemical properties of the compounds and their phloem mobility, the octanol–water partition coefficient (Log*K*ow) and acid dissociation constant (p*K*a) were predicted using the ALOGPS 2.1 program and Chem3D 20.0 software, respectively.

2.6. Antifungal Bioassay In Vitro

The in vitro antifungal activity of the target compounds against the tested pathogenic fungi was determined using the mycelial growth rate inhibition method [35], with PCA as a positive control. First, a calculated amount of each tested compound was dissolved in 0.5 mL of dimethyl sulfoxide (DMSO) and then diluted to 100 mL with sterile water containing 0.1% Tween 80 to prepare a stock solution. Exactly 5 mL of the prepared stock solution of the tested compound was added to 45 mL of sterile PDA medium and mixed thoroughly. The medium was then evenly poured into three 70 mm sterile Petri dishes to form drug-containing agar plates. A 7 mm diameter mycelial plug, cut from a subcultured plate, was inoculated onto the drug-containing medium. The inoculated plates were incubated at 26 ± 2 °C. A medium containing 0.5% DMSO with 0.1% Tween 80 was used as the blank control, and PCA was used as the positive control. Each treatment was performed in triplicate. Once the colony diameter of the blank control reached 55–60 mm, the colony diameter (mm) of each treatment group was accurately measured using the cross-intersection method. The inhibition rate was calculated as follows: Inhibition rate (%) = $[(C - T)/(C - 7\text{ mm})] \times 100$, where C and T represent the colony diameters (mm) on the blank medium and medium with the tested compound, respectively, and 7 mm

is the diameter of the mycelial plug. The growth inhibition rate and standard error were calculated using the Data Processing System (DPS) software (version 20.05).

The EC_{50} values of the tested compounds were determined using the aforementioned method. The inhibition rates of the tested compounds against each fungus were evaluated at 5–7 different concentrations. Finally, the regression curve of logarithmic concentration versus inhibition rate was analyzed using the Data Processing System (DPS) software (version 20.05) to determine the EC_{50} values.

2.7. In Vivo Protective and Curative Activities of Compound **D4** *Against Rice Sheath Blight*

The rice seedlings were cultivated as described in Section 2.2 and used to evaluate the protective and curative activities of the tested compounds against rice sheath blight, with PCA as a positive control. The tested compounds were prepared into solutions at concentrations of 200 μg/mL and 100 μg/mL according to the method described in Section 2.6. The blank control was a 0.1% Tween 80 aqueous solution containing 0.5% DMSO. For the protective activity evaluation, the rice plants were then sprayed with the prepared solutions. After 24 h of treatment, mycelial plugs of *Rhizoctonia solani* were inoculated onto the leaf sheaths of the seedlings. For the curative activity evaluation, inoculation was performed first, followed by spraying the tested compounds 24 h later. After spraying, the treated rice plants were air-dried in a well-ventilated area and subsequently transferred to a greenhouse at 26–30 °C for cultivation. After 14 days, the disease incidence on the inoculated rice seedlings was assessed, and the disease index and control efficacy (%) were calculated. The disease severity grading criteria are provided in Section S7 in the Supporting Information.

2.8. Translocation and Distribution of Compound **D4** *in Tobacco Seedlings*

Experimental design for the uptake and translocation of compound D4 in tobacco seedlings. The systemic translocation and distribution process of compound **D4** in tobacco seedlings was investigated by measuring its content in various plant parts at different time intervals following application to a centrally located treated leaf. A buffer solution containing compound **D4** at a concentration of 400 μmol/L was prepared according to the method described in Section 2.3 and set aside for use. Yellow and withered leaves at the base of the selected tobacco seedlings were removed, while the terminal bud and the middle three pairs of leaves were retained. The plants were divided into six sections, as shown in Figure 4: (i) apical growing point, (ii) stem, (iii) upper leaves, (iv) middle leaves (treated leaves), (v) lower leaves, and (vi) roots. The solution containing 400 μmol/L of compound **D4** was uniformly applied to both sides of the middle tobacco leaves using a soft brush, with care taken to prevent any solution from dripping into the soil or contacting other untreated parts of the plant. At 3 h, 6 h, 12 h, 24 h, and 36 h after treatment, the apical leaves, stem, treated leaf, lower leaves, and roots of the tobacco seedlings were collected (5 g fresh weight per sample) and immediately stored at −20 °C for subsequent extraction and analysis. Each treatment was replicated three times.

Extraction and analysis of compound D4 in tobacco seedlings. The leaf, stem, and root samples collected from tobacco seedlings were thoroughly rinsed with purified water and air-dried. The selected plant tissues were homogenized using a mechanical grinder. To each sample, 10 mL of methanol was added, followed by vortex mixing for 1 min and subsequent ultrasonic extraction for 20 min. Then, 4 g of anhydrous $MgSO_4$, 1 g of NaCl, 1 g of trisodium citrate dihydrate ($C_6H_5Na_3O_7{\cdot}2H_2O$), and 0.5 g of disodium hydrogen citrate sesquihydrate ($C_6H_5Na_2O_7{\cdot}1.5H_2O$) were added. The mixture was vortexed for 1 min and centrifuged at 5000 r/min for 5 min. A 5 mL aliquot of the supernatant was transferred to a 10 mL centrifuge tube, where 600 mg of anhydrous $MgSO_4$, 150 mg of

N-propylethylenediamine (PSA), and 200 mg of C_{18} sorbent were added. After vortexing for 1 min, the tube was centrifuged again at 5000 r/min for 5 min. The supernatant was filtered through a 0.22 μm organic membrane into an injection vial for subsequent analysis. The analytical procedure followed the method described in Section 2.3. The details and results of the spike-recovery tests performed in this study are provided in the Supporting Information.

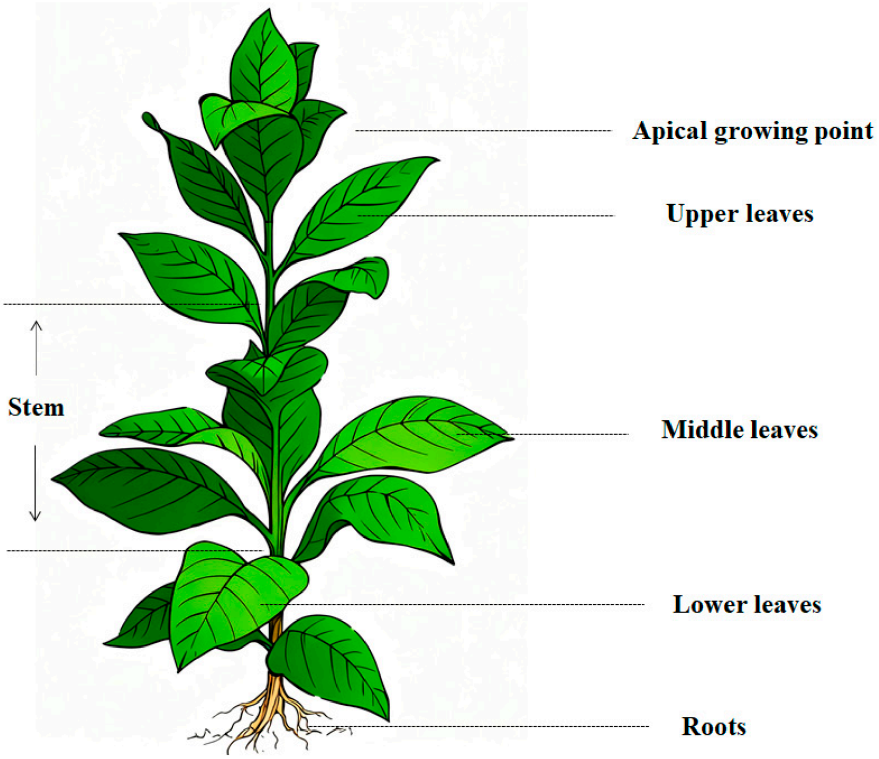

Figure 4. The diagrammatic representation of the tobacco seedling separated into six different sections (1: apical growing point; 2: upper leaves; 3: stem; 4: middle leaves (treated); 5: lower leaves; 6: roots).

3. Results and Discussion

3.1. Phloem Mobility of Nine Heterocyclic Carboxylic Acids **C1**–**C9**

The phloem mobility of nine commercially available heterocyclic carboxylic acids **C1**–**C9** (Figure 5) was evaluated using a *Ricinus communis* system. The linear equations relating the concentration of each compound to its chromatographic peak area, as well as the detected concentrations in the phloem sap, are summarized in Table 1. The results demonstrated that all compounds exhibited phloem mobility except for **C1**, which contains a pyrazole ring and showed no detectable phloem mobility. Among the phloem-mobile compounds, **C8** displayed the highest phloem mobility level, with a concentration of 14.478 μmol/L in the phloem sap, followed by **C7** at 6.904 μmol/L. It is noteworthy that **C5**, **C6**, **C7**, and **C8** are isomers, all of which showed phloem mobility but with distinct mobility capacities. These findings reveal that the phloem mobility of heterocyclic carboxylic acids is influenced not only by the type of heterocycle but also by the position of substituents on the ring. Furthermore, the results suggest the potential of these exogenous heterocyclic carboxylic acids to serve as exogenous vector groups.

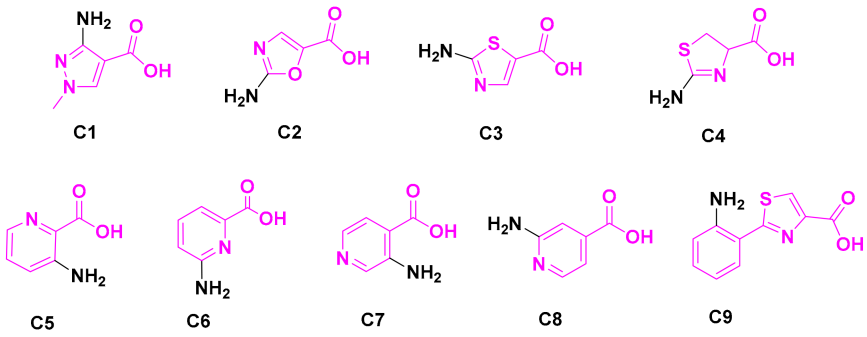

Figure 5. Chemical structures of heterocyclic carboxylic acids **C1**–**C9** evaluated as potential exogenous vector groups.

Table 1. The linear equations of compounds **C1**–**C9** and their concentration in phloem sap.

Compd.	Structures	Linear Equations	R^2	Concentration in Phloem Sap (μmol/L)
C1	2-aminooxazole-5-carboxylic acid	-	-	ND [a]
C2	2-aminooxazole-5-carboxylic acid	$y = -80460.9 + 4327670x$	0.9992	0.828 ± 0.021
C3	2-aminothiazole-5-carboxylic acid	$y = -59365.8 + 3018130x$	0.9999	1.200 ± 0.025
C4	2-amino-4,5-dihydrothiazole-4-carboxylic acid	$y = -7769.49 + 22002.3x$	0.9991	0.305 ± 0.002
C5	3-aminopicolinic acid	$y = -305172 + 633810x$	0.9998	4.193 ± 0.058
C6	6-aminopicolinic acid	$y = 257443 + 454887x$	0.9997	0.502 ± 0.005
C7	3-aminoisonicotinic acid	$y = 80185.6 + 4071150x$	0.9998	6.904 ± 0.085
C8	2-aminoisonicotinic acid	$y = 392925 + 587678x$	0.9992	14.478 ± 0.010
C9	2-(2-aminophenyl)thiazole-4-carboxylic acid	$y = -546338 + 11889600x$	0.9990	2.155 ± 0.033

[a] ND means not detected.

3.2. Chemistry

The synthesis methods and chemical structures of target compounds **D1**–**D9** are shown in Figure 3. In brief, PCA was treated with oxalyl chloride and a catalytic amount of DMF in a CH_2Cl_2 solution under reflux to afford intermediate **B**. Subsequently, the corresponding heterocyclic acid **C** was added to intermediate **B** in a CH_2Cl_2 solution, using triethylamine as the base, to yield the target compound **D**. All target compounds were characterized by ^{1}H NMR, ^{13}C NMR, and HRMS. The physicochemical properties and yields of the target compounds are summarized in Table 2. In terms of appearance, most of the compounds were obtained as yellow or brown solids. Except for compound **D6**, which was obtained in 47.83% yield, the other eight compounds were isolated in yields exceeding 50%, with the majority exhibiting yields above 70%. The spectral data of target compounds are provided in the Supplementary Information.

Table 2. The physicochemical properties and yields of the target compounds.

Compd.	Structures	Molecular Weight (g mol^{-1})	Yield
D1	1-methyl-3-(phenazine-1-carboxamido)-1*H*-pyrazole-4-carboxylic acid	347.33	75.00%
D2	2-(phenazine-1-carboxamido)oxazole-5-carboxylic acid	334.29	52.83%
D3	2-(phenazine-1-carboxamido)thiazole-5-carboxylic acid	350.35	54.29%
D4	2-(phenazine-1-carboxamido)-4,5-dihydrothiazole-4-carboxylic acid	352.37	76.60%
D5	3-(phenazine-1-carboxamido)picolinic acid	344.33	84.78%
D6	6-(phenazine-1-carboxamido)picolinic acid	344.33	47.83%
D7	3-(phenazine-1-carboxamido)isonicotinic acid	344.33	70.59%
D8	2-(phenazine-1-carboxamido)isonicotinic acid	344.33	85.71%
D9	2-(2-(phenazine-2-carboxamido)phenyl)thiazole-4- carboxylic acid	426.45	55.81%

3.3. Phloem Mobility of the Target Compounds **D1**–**D9**

The phloem mobility of the nine target compounds **D1**–**D9** and PCA was evaluated using the *Ricinus communis* system. The results showed that PCA and compounds **D3**, **D5**,

D6, and **D8** were not detected in the phloem sap (indicating no phloem mobility), while the remaining five target compounds (**D1**, **D2**, **D4**, **D7**, and **D9**) exhibited phloem mobility. Their linear equations and detected concentrations are presented in Table 3. Notably, compound **D7** displayed the highest phloem mobility, with a detected concentration of 170.01 μmol/L, followed by **D1** (167.94 μmol/L). Comparing these results with the phloem mobility vector groups (**C1**–**C9**; Table 1) revealed several intriguing observations. For instance, although vector group **C1** exhibited no phloem mobility, its corresponding target compound **D1** exhibited remarkable phloem mobility, with a detected concentration of 167.94 μmol/L in the phloem sap comparable to that of **D7** (170.01 μmol/L), the most phloem-mobile compound. Moreover, the phloem mobility of **D1** was over 10 times higher than that of **C8** (14.478 μmol/L), the vector group with the highest observed phloem mobility. It is also worth noting that the vector groups **C5**, **C6**, **C7**, and **C8** are isomers, all of which exhibited phloem mobility. However, after conjugating them with PCA via an amide bond to form the corresponding target compounds **D5**, **D6**, **D7**, and **D8**, only **D7** retained phloem mobility. The inconsistency between the phloem mobility of the target compounds and their corresponding vector groups may be related to their specific transport mechanisms. Conjugation with PCA markedly changed the physicochemical properties of the heterocyclic carboxylic acids. For example, the LogKow value increased from −0.04 for **C1** to 2.13 for **D1**, while the pKa shifted from 3.292 to 2.817. Similar changes were observed for the pyridinecarboxylic-acid-derived positional analogs **D5**–**D8**. However, the phloem mobility of the free acids did not directly predict that of the corresponding PCA amides. The non-mobile vector group **C1** gave rise to the highly mobile conjugate **D1**, whereas among **D5**–**D8**, only **D7** retained phloem mobility. These results indicate that conjugation not only changes lipophilicity and acidity, but may also alter the spatial arrangement of the heterocyclic moiety, thereby affecting membrane permeation and possible recognition by transport-related proteins.

Table 3. The linear equations of the tested compounds and their concentration in phloem sap.

Compd.	Structures	Linear Equations	R^2	Concentration in Phloem Sap (μmol/L)
D1	1-methyl-3-(phenazine-1-carboxamido)-1*H*-pyrazole-4-carboxylic acid	$y = 578310 + 3473990x$	0.9991	167.94 ± 0.131
D2	2-(phenazine-1-carboxamido)oxazole-5-carboxylic acid	$y = -3988877 + 6086020x$	0.9953	1.716 ± 0.033
D4	2-(phenazine-1-carboxamido)-4,5-dihydrothiazole-4-carboxylic acid	$y = -151884 + 856166x$	0.9994	2.109 ± 0.009
D7	3-(phenazine-1-carboxamido)isonicotinic acid	$y = 606.47 + 663067x$	0.9999	170.01 ± 0.805
D9	2-(2-(phenazine-2-carboxamido)phenyl)thiazole-4- carboxylic acid	$y = -81020.5 + 512986x$	0.9996	12.874 ± 0.117

The Kleier model is a probability distribution map of phloem mobility of compounds constructed based on extensive data derived from known phloem-mobile xenobiotics, with the Log*K*ow and p*K*a as the main parameters. The model predictions showed a high degree of consistency with experimental data from most known phloem-mobile herbicides, fungicides, and insecticides, with the exception of some unique xenobiotics whose transport mechanisms have been confirmed to be carrier-mediated. Therefore, it is generally accepted that phloem-mobile compounds consistent with the Kleier model achieve phloem translocation primarily through passive diffusion or ion-trapping mechanisms.

By integrating the physicochemical properties of the compounds listed in Tables 4 and 5 with the Kleier model diagram, we derived the probability distribution of phloem mobility for these compounds, as illustrated in Figure 6. According to the predictions of the Kleier model, all tested compounds exhibit theoretical potential for phloem mobility, with the exception of **D9**, which is categorized as "non-phloem mobile." Specifically, compound **D8** is in the "very good phloem mobility" range; compounds **D1**, **D2**, **D3**, **D4**, **D5**, **D6**, **D7**, and **C9** belong to the "moderately phloem mobile" range; while the remaining compounds fall into the "possibly phloem mobile" range. However, these predictions are inconsistent with the phloem mobility data obtained from the *Ricinus communis* system (Table 3). For instance,

compounds **D3**, **D5**, and **D6** were predicted to be moderately mobile, and compound **D3** was even predicted to be very mobile, yet the experimentally measured phloem mobility results for these compounds were the opposite—none of them exhibited phloem mobility. Notably, compound **D9** demonstrated phloem mobility experimentally but was predicted by the Kleier model to be non-mobile. These discrepancies suggest that the synthesized target compounds—PCA amides containing heterocyclic carboxylic acids with phloem mobility—in this study may not be absorbed and transported in the castor phloem via the "ion trap" mechanism or passive diffusion. In fact, some recent studies have confirmed that certain plant transporters can facilitate the translocation of exogenous carboxylic acid small molecules [41,42]. For instance, it has been demonstrated that Arabidopsis LAX3 (a key protein involved in root formation) not only has high affinity and transport capacity for IAA but also binds synthetic hormone-like herbicides, such as 2,4-dichlorophenoxyacetic acid (2,4-D), as well as auxin transport inhibitors like 1-naphthoxyacetic acid (1-NOA) and 2-naphthoxyacetic acid (2-NOA). Therefore, it is speculated that the phloem mobility of the target compounds in this study, especially **D9**, may involve carrier-mediated active transport during their absorption and translocation in castor phloem. Further research is required to identify the specific carrier proteins and elucidate their functional roles.

Table 4. Physicochemical properties of vector groups and target compounds and PCA.

Compd.	Log *Kow*	p*Ka*	Compd.	Log *Kow*	p*Ka*
C1	−0.04	3.292	**D1**	2.13	2.817
C2	−0.49	2.125	**D2**	3.05	1.889
C3	0.06	2.967	**D3**	2.56	2.765
C4	−0.83	3.205	**D4**	1.78	2.989
C5	0.23	2.989	**D5**	2.49	2.447
C6	0.43	3.248	**D6**	2.86	3.013
C7	−0.10	3.551	**D7**	1.97	3.076
C8	0.14	3.812	**D8**	2.48	3.577
C9	2.09	3.127	**D9**	4.51	3.016
PCA	2.34	1.59			

Table 5. Antifungal EC_{50} values of tested compounds against pathogenic fungi.

Fungi	Compd.	Regression Equation	EC_{50} (μmol/mL)	95% Confidence Interval (μmol/mL)	R^2
R. solani	**D4**	$y = 4.6663 + 0.8574x$	0.0070	0.0032–0.0153	0.9264
	PCA	$y = 4.8117 + 0.3966x$	0.0133	0.0085–0.0207	0.9746
F. moniliforme	**D4**	$y = 2.9554 + 1.3714x$	0.0879	0.0662–0.1166	0.9891
	PCA	$y = 3.4080 + 1.2813x$	0.0779	0.0619–0.0981	0.9872
B. cinerea	**D4**	$y = 3.1188 + 2.1766x$	0.0208	0.0166–0.0260	0.9863
	PCA	$y = 4.0399 + 1.6469x$	0.0171	0.0140–0.0208	0.9871
P. infestans	**D4**	$y = 4.7343 + 0.9831x$	0.0053	0.0044–0.0063	0.9914
	PCA	$y = 4.8206 + 1.1158x$	0.0065	0.0049–0.0086	0.9822
B. maydis	**D4**	$y = 3.9423 + 1.3632x$	0.0169	0.0112–0.0039	0.9856
	PCA	$y = 4.3231 + 1.2679x$	0.0152	0.0119–0.0196	0.9827
C. camelliae	**D4**	$y = 1.7657 + 2.1448x$	0.0914	0.0779–0.1073	0.9936
	D6	$y = 3.9951 + 0.9342x$	0.0346	0.0242–0.0494	0.9701
	PCA	$y = 2.9825 + 1.6424x$	0.0755	0.0557–0.1022	0.9776
P. oryzae	**D4**	$y = 3.5293 + 1.0742x$	0.0664	0.0400–0.1102	0.9698
	PCA	$y = 3.4797 + 1.2666x$	0.0707	0.0509–0.0982	0.9829

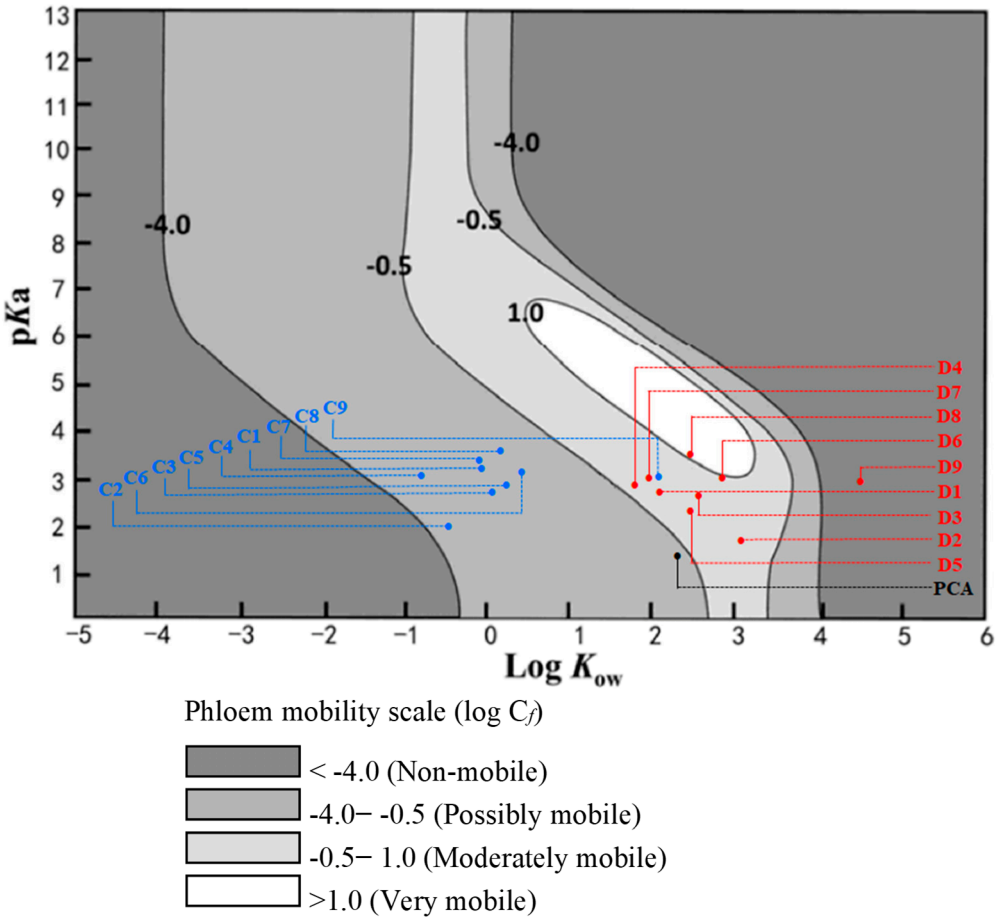

Figure 6. Prediction of the phloem mobility of the tested compounds using the Kleier map (log C_f as a function of p*K*a and Log *K*ow).

3.4. In Vitro Antifungal Activity of the Target Compounds **D1–D9**

The in vitro antifungal activity of the nine target compounds against eight destructive plant pathogenic fungi (*R. solani*, *F. moniliforme*, *P. debaryanum*, *B. cinerea*, *P. infestans*, *B. maydis*, *C. camelliae*, *P. oryzae*) was evaluated at a concentration of 50 μg/mL using the mycelial growth rate method, with PCA as the positive control. The antifungal activity data for all tested compounds are shown in Figure 7. Figure 7 provides a direct comparison of the inhibition rates of all nine target compounds and PCA against eight pathogenic fungi at 50 μg/mL, allowing the overall antifungal profile of **D4** to be readily compared with PCA and the other analogs. The preliminary screening results revealed different inhibition profiles of the target compounds against various pathogenic fungi at 50 μg/mL. Notably, compounds **D4** and **D6** exhibited broad-spectrum antifungal activity, with **D4** displaying >80% inhibition against most tested fungal strains. In terms of the heterocyclic carboxylic acid type present in the chemical structures of the target compounds, the results indicate that compound **D4**, which contains thiazoline carboxylic acid, demonstrated the best antifungal activity along with broad-spectrum efficacy. Comparing the antifungal activities of compounds **D5**, **D6**, **D7**, and **D8**, which contain isomeric pyridine carboxylic acid, it was found that only compound **D6** partially retained the antifungal activity of the parent PCA, while compounds **D7** and **D8** exhibited near-complete loss of antifungal activity. These results suggest that the antifungal activity of the target compounds is not only related to the type of heterocyclic carboxylic acid but also significantly influenced by the position of substituents.

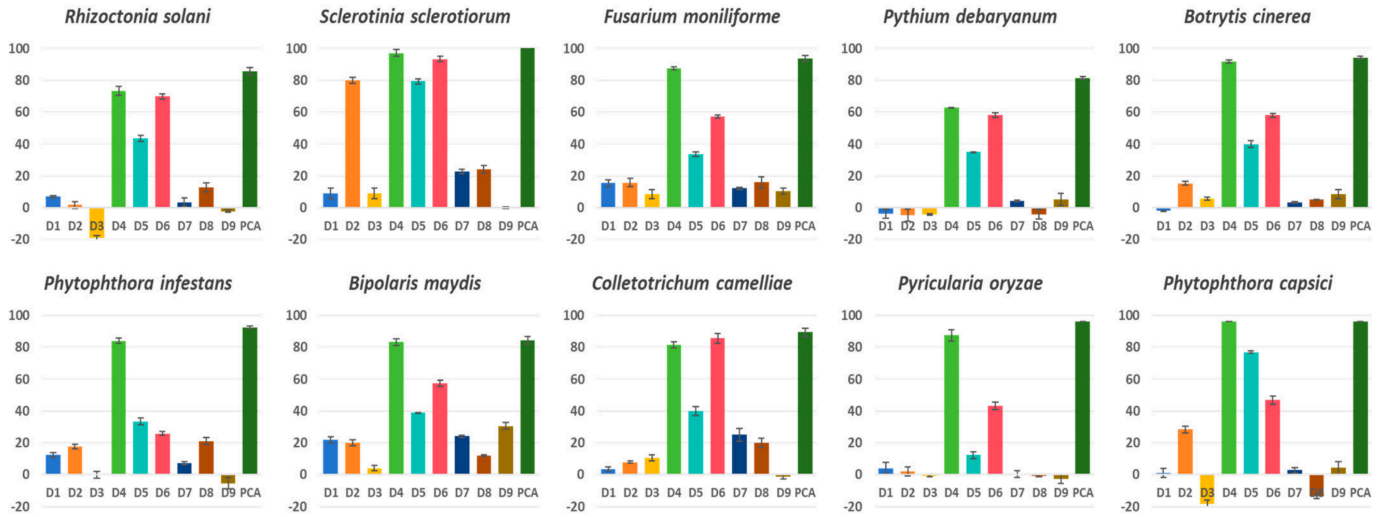

Figure 7. The in vitro inhibition rates of the tested compounds against eight pathogenic fungi at a concentration of 50 μg/mL. (The data are presented as the mean ± SE of three replicates, and the error bars indicate SE.)

The target compounds that exhibited more than 70% inhibitory activity against the tested pathogenic fungi at 50 μg/mL were selected for the determination of EC_{50} values to enable a more accurate comparison of their antifungal efficacy. The EC_{50} values of the compounds against the pathogenic fungi are presented in Table 5. The results indicated that compound **D4** exhibited exceptionally significant antifungal activity against *R. solani*, *P. infestans*, and *P. oryzae* superior to that of the parent compound PCA, with EC_{50} values of 0.0070 μmol/mL, 0.0053 μmol/mL, and 0.0664 μmol/mL, respectively, all of which were lower than those of PCA. Furthermore, **D4** also demonstrated potent antifungal activity against four other fungal species. Notably, compound **D6** showed outstanding antifungal activity against *C camelliae*, with an EC_{50} value of 0.0346 μmol/mL—approximately twice the activity of PCA (EC_{50} = 0.0755 μmol/mL). The bioassay results of EC_{50} further confirmed that the target compound **D4** largely retains the broad-spectrum antifungal activity of the parent PCA while demonstrating enhanced inhibitory efficacy against certain fungi.

3.5. In Vivo Protective and Curative Effects Against Rice Sheath Blight

Among the nine target compounds, compound **D4** exhibited superior in vitro antifungal activity and certain phloem mobility; thus, it was selected for further evaluation of its in vivo protective and curative effects against *R. solani* (rice sheath blight) in pot experiments. As shown in Figure 8, 14 days after inoculation, the control group exhibited dense elliptical lesions at the base of rice plants, with water-soaked brown margins, yellowish-brown stems, and chlorotic, whitened leaves. In contrast, the **D4**-treated group showed significantly fewer and smaller lesions on the rice basal stems, with most parts of the stems retaining normal green coloration. The PCA-treated group, compared to the D4 group, had more lesions, larger lesion areas, and more extensive leaf yellowing. Disease severity assessment and efficacy calculation further confirmed that compound **D4** possesses superior in vivo protective and curative activity against *R. solani* compared to PCA.

As illustrated in Table 6, compound **D4** displayed better in vivo protective and curative activities against *R. solani* than **PCA**. For example, treatment with compound **D4** at the concentrations of 200 and 100 μg/mL resulted in 74.91% and 50.19% protective efficacies after 14 days of transplantation, respectively. However, the protective activities of PCA reached 66.42 and 43.55% at the concentrations of 200 and 100 μg/mL, respectively. In terms of the curative effect against *R. solani*, at the concentrations of 200 and 100 μg/mL,

compound **D4** displayed a slight improvement in vivo curative activity (57.35 and 39.07%, respectively) compared to PCA (50.18 and 37.28%, respectively). Therefore, compound **D4** exhibited superior in vivo protective and curative activities against *R. solani* compared to PCA and could effectively control rice sheath blight. Since rice sheath blight primarily infects the stem base, the phloem mobility of **D4** may explain its enhanced control efficiency in whole-plant efficacy tests. Although the in vitro inhibitory effect of **D4** against *R. solani* was only slightly better than PCA, its in vivo efficacy was significantly stronger. This suggests that **D4** may effectively translocate through the phloem and accumulate in the stem base, thereby improving its control efficiency.

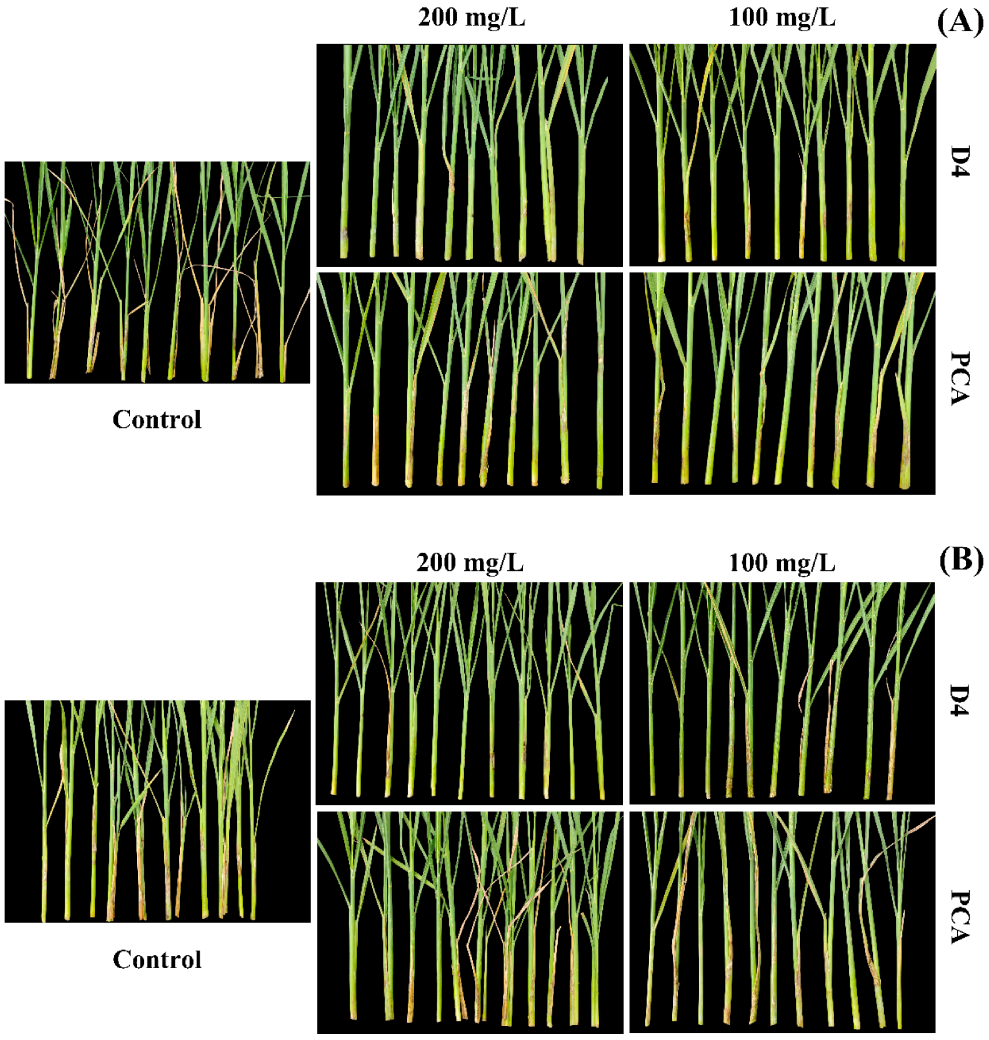

Figure 8. The in vivo protective and curative effects of the tested compounds against *R. solani*. Protective effect (**A**), curative effect (**B**).

Table 6. The in vivo protective and curative effects of the tested compounds against *R. solani*.

Treatment	Concentration (μg/mL)	Control Efficacy (%)	
		Protective Effect	Curative Effect
D4	200	74.91 ± 1.69 a	57.35 ± 0.62 a
	100	50.19 ± 1.11 c	39.07 ± 0.62 c
PCA	200	66.42 ± 1.69 b	50.18 ± 1.64 b
	100	43.55 ± 1.11 d	37.28 ± 2.24 c

Note: Different lowercase letters indicate significant differences ($p < 0.05$) between treatments.

3.6. Translocation and Distribution of Compound D4 in Tobacco Seedlings

Given the phloem mobility and potent in vivo antifungal activity exhibited by the target compound **D4**, we further investigated its translocation and distribution within tobacco seedlings. The content of compound **D4** was analyzed in various parts of tobacco seedlings, including the apical growing point, upper leaves, treated leaves, lower leaves, stems, and roots, at different time intervals following foliar application of compound **D4** on middle tobacco leaves (treated leaves), using HPLC-MS/MS. The results are presented in Figure 9. The results demonstrated that compound D4 was rapidly absorbed by tobacco leaves within 2 h after treatment and efficiently translocated to different parts of the plant. Overall, the highest accumulation of D4 was observed in the roots, followed by the stems, suggesting that **D4** exhibits strong phloem mobility and is capable of basipetal translocation. Similarly, the presence of D4 was also detected in the apical growing point, indicating that it can acropetally translocate through the xylem. Over time, the content of compound **D4** in all parts showed an initial increase followed by a decrease, reaching a relatively stable level between 24 h and 36 h. The spike-recovery results showed that the recovery rates of D4 in tobacco foliage, stems, and roots were 74.19–77.13%, 71.25–108.17%, and 73.03–73.67%, respectively, indicating that the analytical method was suitable for quantifying D4 in tobacco tissue samples. Under the UHPLC-MS/MS conditions used for tissue-distribution analysis, the measured signal was attributed to the parent compound D4.

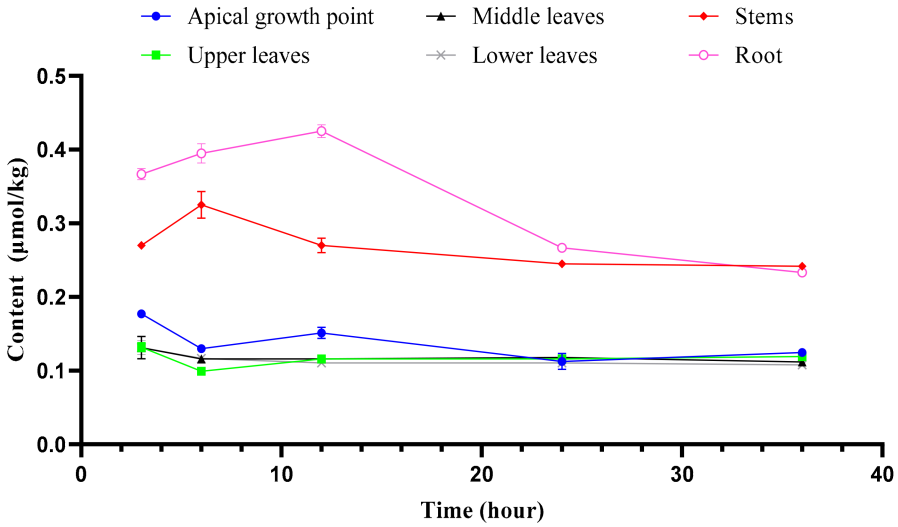

Figure 9. Time-dependent distribution of compound **D4** (400 μmol/L) in different parts of tobacco seedlings after foliar application to middle leaves.

In our previous study, it was found that the amino acid conjugate PCA-L-Val exhibits excellent systemic mobility. The experimental results revealed that the uptake and translocation of PCA-L-Val in castor plants involve an active transport mechanism mediated by amino acid carriers, including the amino acid transporters RcAAP2, RcANT7, and RcLHT1 [36]. Further systemic experiments in tobacco demonstrated that PCA-L-Val can be effectively absorbed through tobacco leaves and translocated throughout the entire plant, enabling systemic disease control [19]. In the current study, using exogenous heterocyclic carboxylic acids as vector groups, we successfully obtained excellent antifungal compounds with phloem mobility, such as compound **D4**. Similarly, this compound can be absorbed through tobacco leaves and transported to various parts of the plant, with significant accumulation observed particularly in the roots and stems. In the in vivo bioassays against rice sheath blight, compound **D4** also demonstrated comprehensively superior control efficacy

compared to PCA. These findings highlight that the systemic properties of compound **D4** contribute to enhanced efficacy against root and vascular diseases.

4. Conclusions

In summary, we report a pesticide vectorization strategy using exogenous compounds as vector groups. Nine novel PCA amide derivatives containing heterocyclic carboxylic acids were designed and synthesized, and their structures were characterized by ^{1}H NMR, ^{13}C NMR, and HRMS. All target compounds exhibited certain in vitro antifungal activities against the tested pathogens. In particular, compound **D4** showed excellent broad-spectrum antifungal activity with enhanced efficacy against certain pathogens compared to PCA. Phloem mobility tests in the *Ricinus communis* system demonstrated that the five target compounds **D1**, **D2**, **D4**, **D7**, and **D9** exhibited phloem mobility, likely via carrier-mediated active transport. The pot experiment results confirmed that compound **D4** had superior protective and curative efficacy against rice sheath blight compared to PCA, which may be attributed to its phloem mobility. Further systemic studies in tobacco revealed that compound **D4** can be absorbed by leaves and translocated throughout the entire plant, with a notable tendency to accumulate in the roots and stems. This contributes to the efficacy of compound **D4** in controlling root and vascular diseases. Hence, these present results offer a new strategy for pesticide vectorization and provide data support for the development of phloem-mobile pesticides with enhanced bioactivity.

Supplementary Materials: The following supporting information can be downloaded at https://www.mdpi.com/article/10.3390/agronomy16181762/s1: ^{1}H NMR, ^{13}C NMR, and HRMS spectrum of the compounds are shown in Supporting Information.

Author Contributions: Conceptualization, X.Z. and J.L.; methodology, X.Z., Y.T., G.M. and T.Y.; formal analysis, X.Z., Q.H. and L.Y.; investigation, X.Z., L.L., T.Y., G.M. and Y.T.; writing—original draft preparation, L.L., X.Z. and J.L.; writing—review and editing, Y.T., X.Z. and J.L.; supervision, J.L. and X.Z.; funding acquisition, J.L. and X.Z.; project administration, J.L. All authors have read and agreed to the published version of the manuscript.

Funding: This work was supported by the China Postdoctoral Science Foundation (2022M710917), the National Natural Science Foundation of China (32302417), the Natural Science Foundation of Hubei Province (2023AFB287) and the Open Fund of Engineering Research Center of Ecology and Agricultural Use of Wetland, Ministry of Education (KF202304).

Data Availability Statement: The original contributions presented in this study are included in the article/Supplementary Material. Further inquiries can be directed to the corresponding authors.

Conflicts of Interest: The authors declare no competing financial interest.

References

1. Ma, H.; Wang, K.; Wang, B.; Wang, Z.; Liu, Y.; Wang, Q. Design, synthesis, and biological activities of novel coumarin derivatives as pesticide candidates. *J. Agric. Food Chem.* **2024**, *72*, 4658–4668. [CrossRef] [PubMed]
2. Song, X.; Wang, H.; Zou, W.; Hong, H.; Gao, Y.; Zhao, C.; Xu, H.; Yao, G. New isoxazoline cyclopropyl-picolinamide derivatives as potential insecticides. *J. Agric. Food Chem.* **2025**, *73*, 6589–6598. [CrossRef] [PubMed]
3. Guo, X.; Wang, H.; Zhao, B.; Fan, Z.; He, L. Synthesis and fungicidal evaluation of novel 2-phenyl thiazole derivatives. *Pestic. Biochem. Physiol.* **2025**, *215*, 106668. [CrossRef] [PubMed]
4. Yao, G.; Zhu, C.; Qin, T.; Wang, M.; Sun, Z.; Tang, R.-Y.; Zhao, C.; Jiang, H.; Xu, H. Oxidative Annulation of Aldehydes, 5-Aminopyrazoles, and Nitriles: Synthesis and Applications of Pyrazolo[3,4-d]Pyrimidines. *Adv. Synth. Catal.* **2023**, *365*, 1191–1204. [CrossRef]
5. Huang, D.; Qi, H.; Liu, H.; Yuan, F.; Yang, C.; Liu, T. Two birds with one stone: Eco-friendly nano-formulation endows a commercial fungicide with excellent insecticidal activity. *Adv. Funct. Mater.* **2025**, *35*, 202420401. [CrossRef]
6. Guo, Z.; Cai, D.; Bai, J.; Xu, T.; Yu, F. Intelligent rice field weed control in precision agriculture: From weed recognition to variable rate spraying. *Agronomy* **2024**, *14*, 1702. [CrossRef]

7. Li, X.; Giles, D.K.; Niederholzer, F.J.; Andaloro, J.T.; Lang, E.B.; Watson, L.J. Evaluation of an unmanned aerial vehicle as a new method of pesticide application for almond crop protection. *Pest Manag. Sci.* **2021**, *77*, 527–537. [CrossRef] [PubMed]
8. Zhang, X.; Li, Z. Generalizing routes of plant exposure to pesticides by plant uptake models to assess pesticide application efficiency. *Ecotoxicol. Environ. Saf.* **2023**, *262*, 12. [CrossRef] [PubMed]
9. Wang, P.; Hanif, A.S.; Yu, S.H.; Lee, C.G.; Kang, Y.H.; Lee, D.H.; Han, X. Development of an autonomous drone spraying control system based on the coefficient of variation of spray distribution. *Comput. Electron. Agric.* **2024**, *227*, 109529. [CrossRef]
10. Li, L.; Hu, Z.; Liu, Q.; Yi, T.; Han, P.; Zhang, R.; Pan, L. Effect of flight velocity on droplet deposition and drift of combined pesticides sprayed using an unmanned aerial vehicle sprayer in a peach orchard. *Front. Plant Sci.* **2022**, *13*, 981494. [CrossRef] [PubMed]
11. Chollet, J.-F.; Rocher, F.; Jousse, C.; Delétage-Grandon, C.; Bashiardes, G.; Bonnemain, J.-L. Synthesis and phloem mobility of acidic derivatives of the fungicide fenpiclonil. *Pest Manag. Sci.* **2004**, *60*, 1063–1072. [CrossRef] [PubMed]
12. Niu, J.; Nie, D.; Yu, D.; Wu, Q.; Yu, L.; Yao, Z.; Du, X.; Li, J. Synthesis, fungicidal activity and phloem mobility of phenazine-1-carboxylic acid-alanine conjugates. *Pestic. Biochem. Physiol.* **2017**, *143*, 8–13. [CrossRef] [PubMed]
13. Cohen, Y.; Weitman, M. Mobility of oxathiapiprolin in and between tomato plants. *Pest Manag. Sci.* **2023**, *79*, 1102–1112. [CrossRef] [PubMed]
14. Wu, Y.; Mao, G.; Xing, G.; Tian, Y.; Hu, Y.; Liao, C.; Li, L.; Zhu, X.; Li, J. Study on the Design, Synthesis, Bioactivity and Translocation of the Conjugates of Phenazine-1-carboxylic Acid and *N*-Phenyl Alanine Ester. *Molecules* **2024**, *29*, 1780. [CrossRef] [PubMed]
15. Brück, E.; Elbert, A.; Fischer, R.; Krueger, S.; Kühnhold, J.; Klueken, A.M.; Nauen, R.; Niebes, J.-F.; Reckmann, U.; Schnorbach, H.-J.; et al. Movento®, an innovative ambimobile insecticide for sucking insect pest control in agriculture: Biological profile and field performance. *Crop Prot.* **2009**, *28*, 838–844. [CrossRef]
16. Ponce-Cabrera, L.; Ponce-Flores, A.; Flores-Reyes, T.; Ponce-Flores, E. Selective Wax Cuticle Removal Using Green Wavelength Lasers: A Non-Invasive Method for Enhancing Foliar Uptake. *AgriEngineering* **2025**, *7*, 119. [CrossRef]
17. Tredenick, E.C.; Farrell, T.W.; Forster, W.A. Mathematical Modelling of Hydrophilic Ionic Fertiliser Diffusion in Plant Cuticles: Lipophilic Surfactant Effects. *Plants* **2019**, *8*, 202. [CrossRef] [PubMed]
18. Files, M.C.; Viana, V.E.; Camargo, E.R.; Silva, R.S.; Vieira, L.M.; Kruse, N.D.; Jacobsen, L.R.; Avila, L.A. S-metolachlor in pre-emergence reduces the leaf cuticular wax and increases the efficiency of glyphosate. *Pest Manag. Sci.* **2025**, *81*, 1478–1486. [CrossRef] [PubMed]
19. Zhu, X.; Zhang, M.; Xiao, Y.; Hsiang, T.; Hu, C.; Li, J. Systemic fungicidal activity of phenazine-1-carboxylic acid-valine conjugate against tobacco sore shin and its translocation and accumulation in tobacco (*Nicotiana tabacum* L.). *Pest Manag. Sci.* **2022**, *78*, 1117–1127. [CrossRef] [PubMed]
20. Wan, Q.; Li, Y.; Cheng, J.; Wang, Y.; Ge, J.; Liu, T.; Ma, L.; Li, Y.; Liu, J.; Zhou, C.; et al. Two aquaporins; PIP1;1 and PIP2;1, mediate the uptake of neonicotinoid pesticides in plants. *Plant Commun.* **2024**, *5*, 100830. [CrossRef] [PubMed]
21. Afzal, S.; Singh, N.K.; Lal, A.F.; Sohrab, S.; Singh, N.; Gupta, P.S.; Mishra, S.K.; Adeel, M.; Faizan, M. Nanostructure and plant uptake: Assessing the ecological footprint and root-to-leaf dynamics. *Plant Nano Biol.* **2024**, *10*, 100122. [CrossRef]
22. Grayson, B.T.; Kleier, D.A. Phloem mobility of xenobiotics. IV. modelling of pesticide movement in plants. *Pestic. Sci.* **1990**, *30*, 67–79. [CrossRef]
23. Kleier, D.A. Phloem mobility of xenobiotics. V. structural requirements for phloem-systemic pesticides. *Pestic. Sci.* **1994**, *42*, 1–11. [CrossRef]
24. Brudenell, A.J.P.; Baker, D.A.; Grayson, B.T. Phloem mobility of xenobiotics: Tabular review of physicochemical properties governing the output of the Kleier model. *Plant Growth Regul.* **1995**, *16*, 215–231. [CrossRef]
25. Wu, H.; Hu, P.; Xu, Y.; Xiao, C.; Chen, Z.; Liu, X.; Jia, J.; Xu, H. Phloem Delivery of Fludioxonil by Plant Amino Acid Transporter-Mediated Polysuccinimide Nanocarriers for Controlling Fusarium Wilt in Banana. *J. Agric. Food Chem.* **2021**, *69*, 2668–2678. [CrossRef] [PubMed]
26. Delétage-Grandon, C.; Chollet, J.-F.; Faucher, M.; Rocher, F.; Komor, E.; Bonnemain, J.-L. Carrier-mediated uptake and phloem systemy of a 350-dalton chlorinated xenobiotic with an α-amino acid function. *Plant Physiol.* **2001**, *125*, 1620–1632. [CrossRef] [PubMed]
27. Golla, V.K.; Benz, R.; Kleinekathöfer, U.; Piselli, C. Glyphosate uptake pathway across the outer membrane of *Pseudomonas aeruginosa*. *Biochim. Biophys. Acta (BBA)-Gen. Subj.* **2026**, *11*, 130991.
28. Hart, J.J.; Ditomaso, J.M.; Linscott, D.L.; Kochian, L.V. Transport interactions between paraquat and polyamines in roots of intact maize seedlings. *Plant Physiol.* **1992**, *99*, 1400–1405. [CrossRef] [PubMed]
29. Wu, H.; Xu, H.; Marivingt-Mounir, C.; Bonnemain, J.-L.; Chollet, J.-F. Vectorizing agrochemicals: Enhancing bioavailability via carrier-mediated transport. *Pest Manag. Sci.* **2019**, *75*, 1507–1516. [CrossRef] [PubMed]
30. Dufaud, A.; Chollet, J.-F.; Rudelle, J.; Miginiac, L.; Bonnemain, J.-L. Derivatives of pesticides with an α-amino acid function: Synthesis and effect on threonine uptake. *Pestic. Sci.* **1994**, *41*, 297–304. [CrossRef]

31. Bartholomew, D.M.; Dyk, D.E.V.; Lau, S.-M.C.; O'Keefe, D.P.; Rea, P.A.; Viitanen, P.V. Alternate energy-dependent pathways for the vacuolar uptake of glucose and glutathione conjugates. *Plant Physiol.* **2002**, *130*, 1562–1572. [CrossRef] [PubMed]
32. Yang, W.; Wu, H.-X.; Xu, H.-H.; Hu, A.-L.; Lu, M.-L. Synthesis of glucose-fipronil conjugate and its phloem mobility. *J. Agric. Food Chem.* **2011**, *59*, 12534–12542. [CrossRef] [PubMed]
33. Wu, H.-X.; Yang, W.; Zhang, Z.-X.; Huang, T.; Yao, G.-K.; Xu, H.-H. Uptake and phloem transport of glucose-fipronil conjugate in *Ricinus communis* involve a carrier-mediated mechanism. *J. Agric. Food Chem.* **2012**, *60*, 6088–6094. [CrossRef] [PubMed]
34. Yu, L.; Huang, D.; Zhu, X.; Zhang, M.; Yao, Z.; Wu, Q.; Xu, Z.; Li, J. Design, synthesis; phloem mobility, and bioactivities of a series of phenazine-1-carboxylic acid-amino acid conjugates. *Molecules* **2018**, *23*, 2139. [CrossRef] [PubMed]
35. Zhu, X.; Yu, L.; Hsiang, T.; Huang, D.; Xu, Z.; Wu, Q.; Du, X.; Li, J. The influence of steric configuration of phenazine-1-carboxylic acid-amino acid conjugates on fungicidal activity and systemicity. *Pest Manag. Sci.* **2019**, *75*, 3323–3330. [CrossRef] [PubMed]
36. Xiao, Y.; Wei, X.; Hu, C.; Hsiang, T.; Yin, J.; Li, J. Multiple amino acid transporters as carriers load l-valine-phenazine-1-carboxylic acid conjugate into *Ricinus* sieve tubes for the phloem translocation. *Int. J. Biol. Macromol.* **2024**, *257*, 128730. [CrossRef] [PubMed]
37. Yang, J.; Ye, T.; Liu, G.; Xu, X.; Zheng, Y.; Wang, W. Synthesis and bioactivity of indoleacetic acid-carbendazim and its effects on *Cylindrocladium parasiticum*. *Pestic. Biochem. Physiol.* **2019**, *158*, 128–134. [CrossRef] [PubMed]
38. Chamberlain, K.; Tench, A.-J.; Williams, R.-H.; Bromilow, R.-H. Phloem translocation of pyridinecarboxylic acids and related imidazolinone herbicides in *Ricinus communis*. *Pestic. Sci.* **1995**, *45*, 69–75. [CrossRef]
39. Satchivi, N.-M.; Stoller, E.-W.; Wax, L.-M.; Briskin, D.P.-A. Nonlinear dynamic simulation model for xenobiotic transport and whole plant allocation following foliar application. II. model validation. *Pestic. Biochem. Physiol.* **2000**, *68*, 85–95. [CrossRef]
40. Bukun, B.; Gaines, T.-A.; Nissen, S.-J.; Westra, P.; Brunk, G.; Shaner, D.-L.; Sleugh, B.-B.; Peterson, V.-F. Aminopyralid and clopyralid absorption and translocation in Canada thistle (*Cirsium arvense*). *Weed Sci.* **2009**, *57*, 10–15. [CrossRef]
41. Tan, S.; Zhang, X.; Kong, W.; Yang, X.-L.; Molnár, G.; Vondráková, Z.; Filepová, R.; Petrášek, J.; Friml, J.; Xue, H.-W. The lipid code-dependent phosphoswitch PDK1–D6PK activates PIN-mediated auxin efflux in *Arabidopsis*. *Nat. Plants* **2020**, *6*, 556–569. [CrossRef] [PubMed]
42. Ung, K.-L.; Schulz, L.; Zuzic, L.; Amsinck, B.-L.; Koutnik-Abele, S.; Benhammouche, I.; Andersen, C.-G.; Nel, L.; Schiøtt, B.; Stokes, D.-L.; et al. Structures and mechanism of the AUX/LAX transporters involved in auxin import. *Nat. Plants* **2025**, *11*, 1670–1680. [CrossRef] [PubMed]